Design of Novel Solid-State Electrolytes Based on Plastic Crystals of Quinuclidinolium Methanesulfonate for Proton Conduction

Samet Ocak,[‡,a] *Federico Poli,*[‡,a] *Dario Braga,*[a] *Tommaso Salzillo,*[*b,c] *Fabrizio Tarterini,*[b] *Gianluca Carì,*[a] *Elisabetta Venuti,*[b] *Francesca Soavi,*[*a] *and Simone d'Agostino*[*a]

[a] Department of Chemistry "Giacomo Ciamician" Alma Mater Studiorum – University of Bologna. Via F. Selmi, 2, 40126 Bologna, Italy

[b] Department of Industrial Chemistry "Toso Montanari" Alma Mater Studiorum – University of Bologna. Viale del Risorgimento 4, 40124, Bologna, Italy.

[c] Department of Chemical and Biological Physics Weizmann Institute of Science Rehovot 76100, Israel.

Electronic Supporting Information (10 pages)

Table of contents

Table S1. Crystal data and refinement details for crystalline [QHco]MS, [QHrac]MS, and R-[QH]MS.

	[QHco]MS	**[QHrac]MS**	**R-[QH]MS**
Formula	$C_8H_{15}NO_4S$	$C_8H_{17}NO_4S$	$C_8H_{17}NO_4S$
FW (g/mol)	221.276	223.291	223.291
Temperature/K	300	300	100
Crystal System	Orthorhombic	Monoclinic	Orthorhombic
Space Group	Pnma	$P2_1/c$	$P2_12_12_1$
a/Å	20.1416(6)	12.0460(8)	9.2714(3)
b/Å	8.3568(2)	9.6190(6)	9.5306(3)
c/Å	6.3468(2)	9.1390(6)	11.8023(5)
α/°	90	90	90
β/°	90	96.107(2)	90
γ/°	90	90	90
Volume/Å^3	1068.29(6)	1052.94(12)	1042.87(6)
Z	4	4	4
ρcalc g/cm^3	1.376	1.409	1.422
μ/mm^{-1}	0.269	0.268	0.301
measd rflns	258	454	3934
indep rflns	-	-	2360
R_1	-	-	0.0646
wR_2	-	-	0.1462
Rwp	4.2	9.8	-

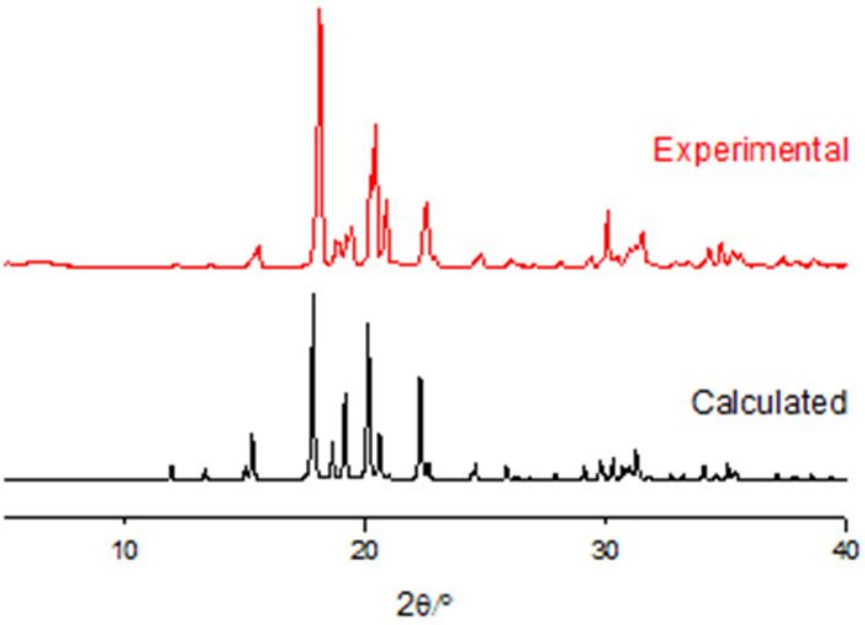

Figure S1. Comparison between calculated (black-line) and experimental (red-line) powder XRD patterns collected at RT for R-[QH]MS.

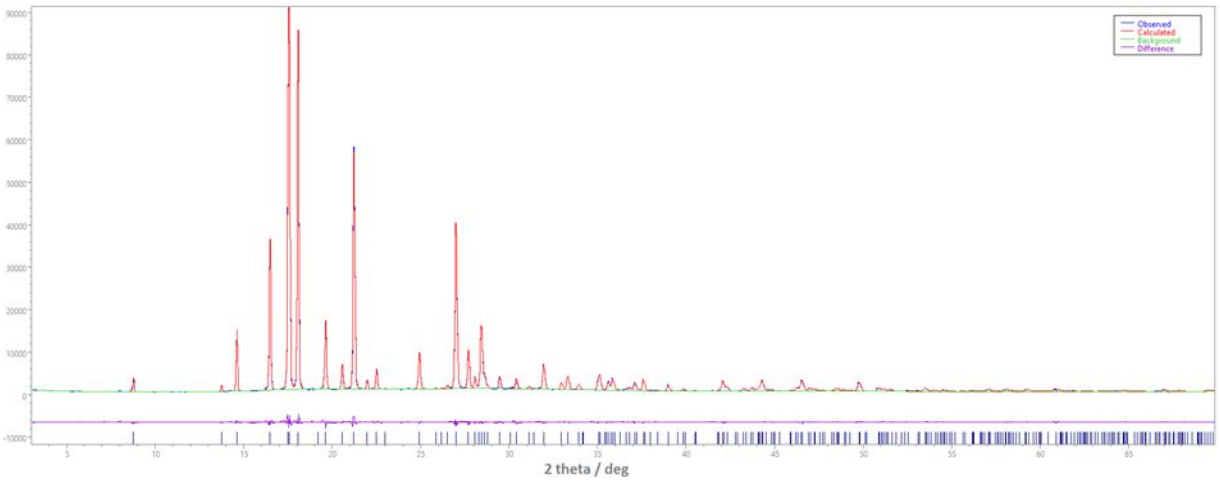

Figure S2. Experimental (blue), calculated (red) powder XRD pattern of [QHco]MS by Rietveld refinement and difference profile (magenta).

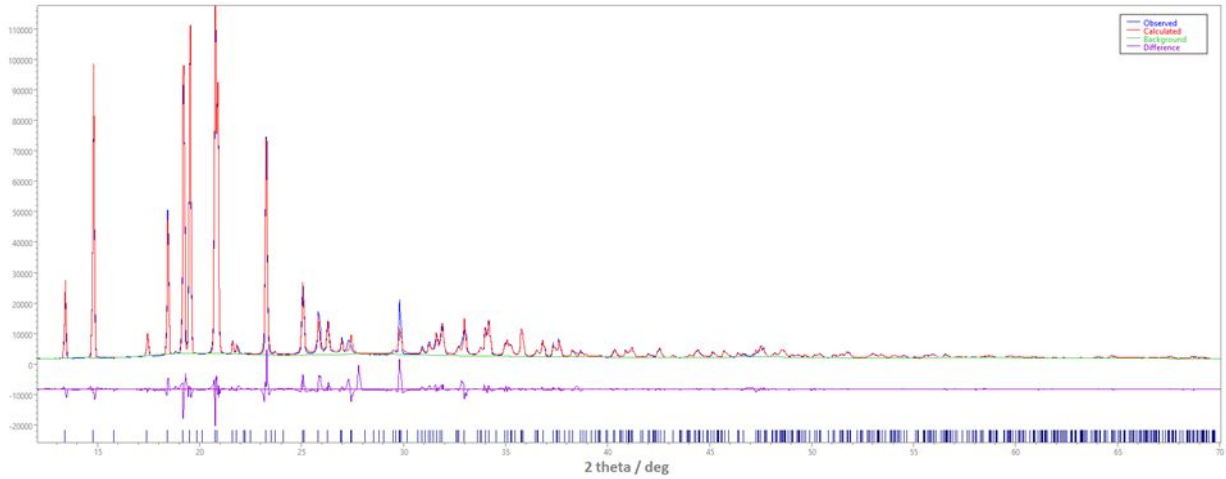

Figure S3. Experimental (blue), calculated (red) powder XRD pattern of [QHrac]MS by Rietveld refinement and difference profile (magenta).

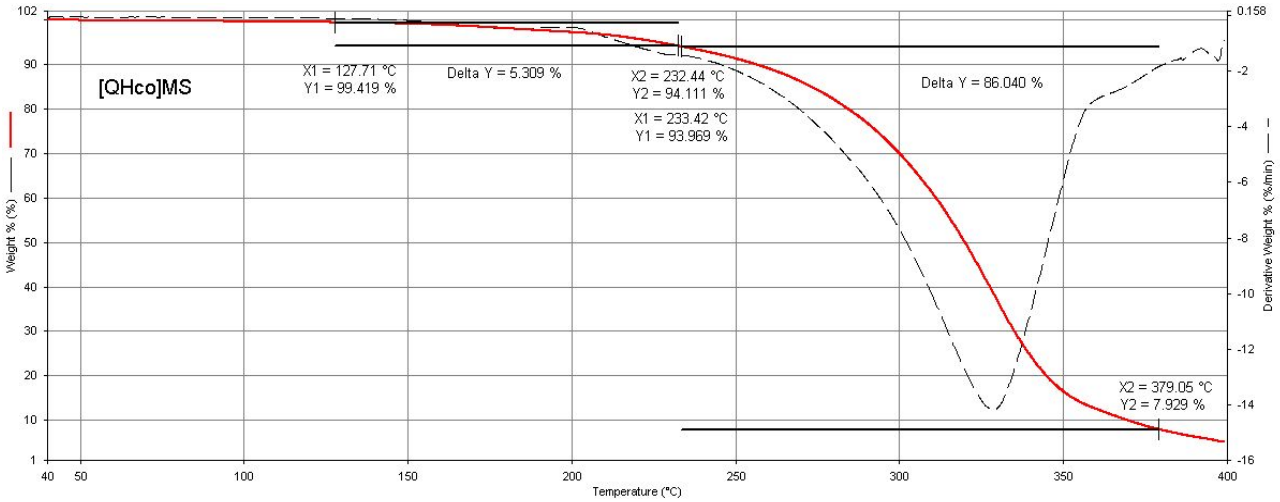

(a)

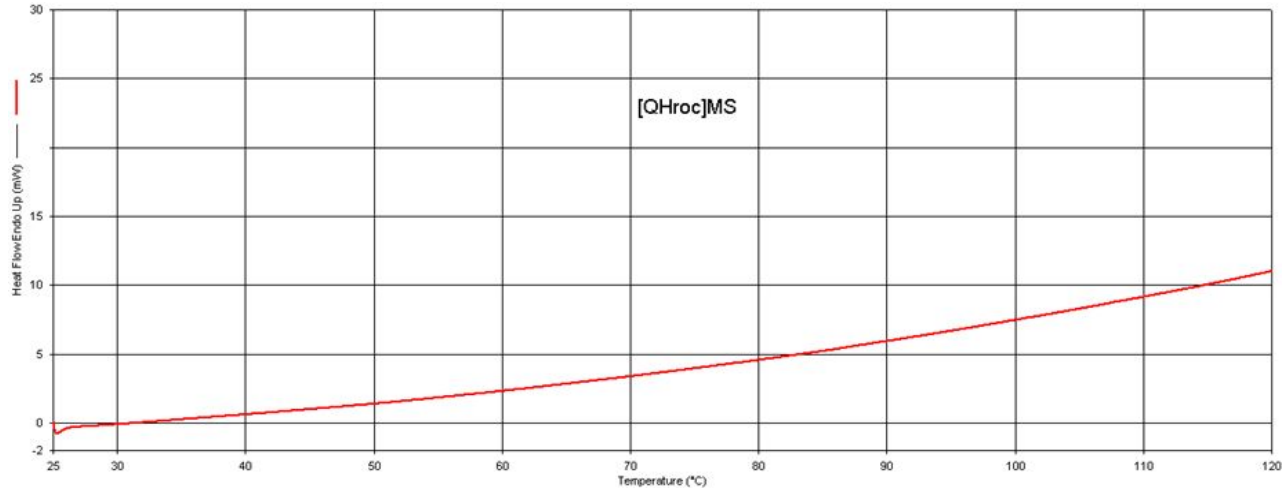

(b)

Figure S4. Thermal analyses for [QHco]MS: (a) TGA thermogram and (b) DSC, heating cycle.

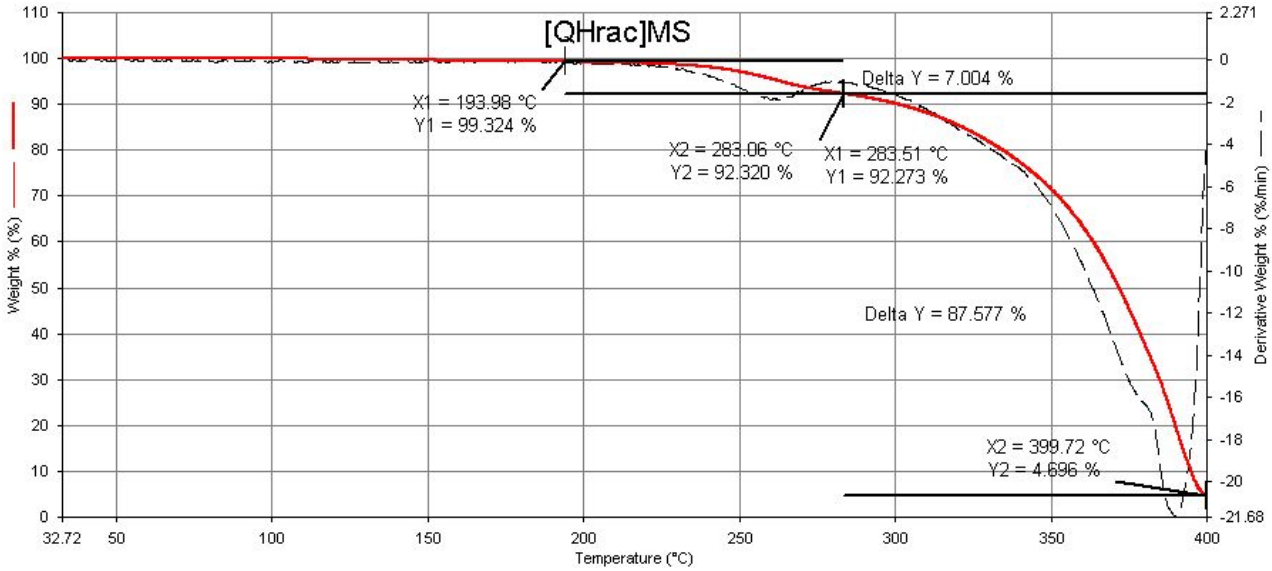

(a)

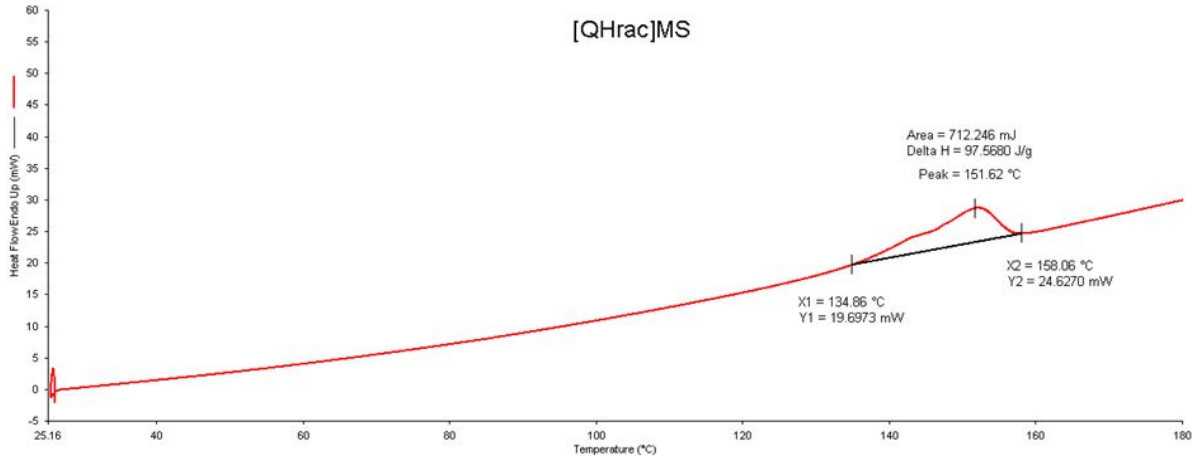

(b)

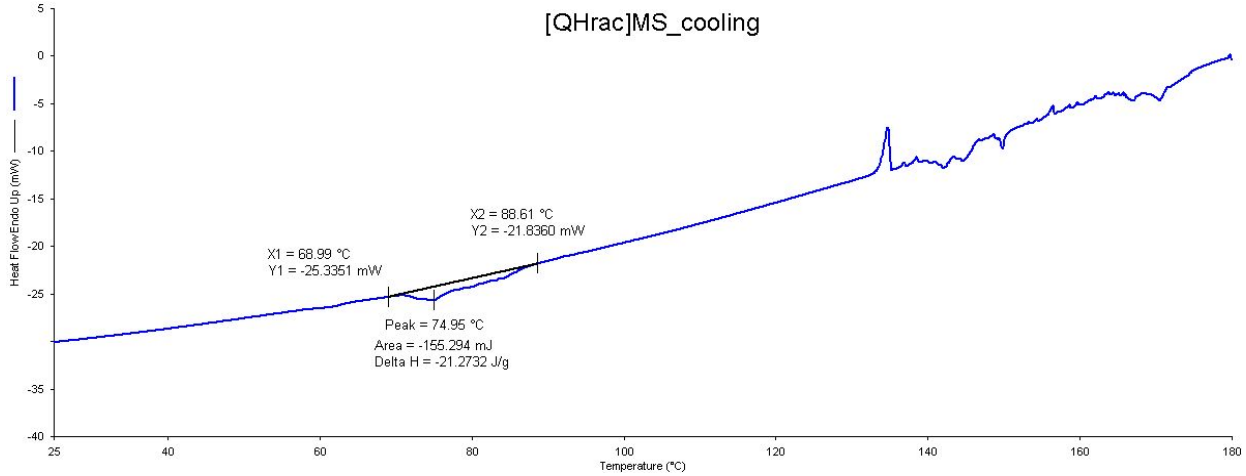

(c)

Figure S5. Thermal analyses for [QHrac]MS: (a) TGA thermogram, (b) DSC, heating cycle and (c) DSC trace, cooling cycle.

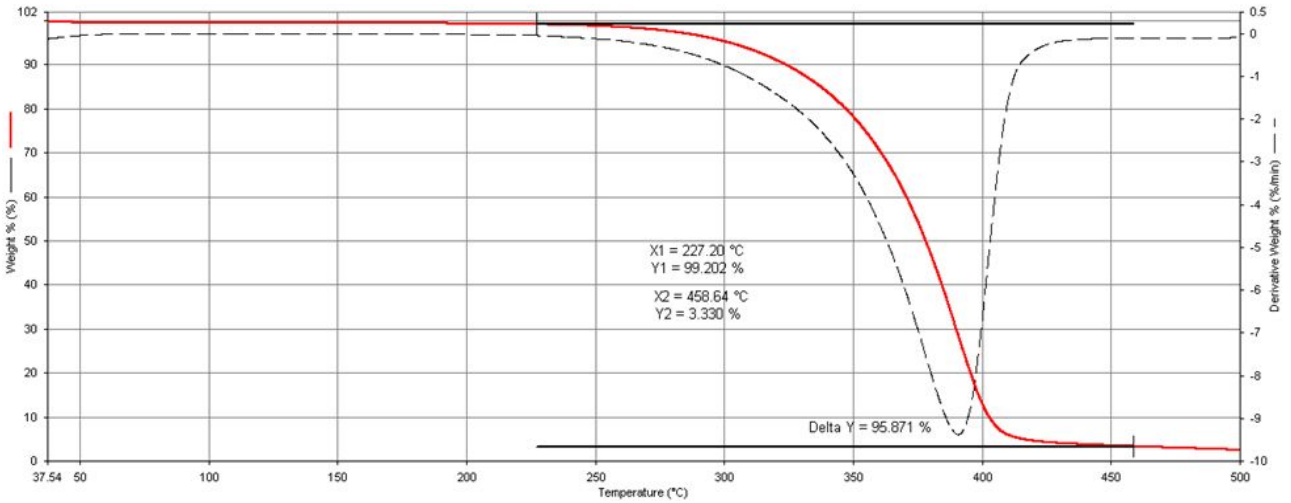

(a)

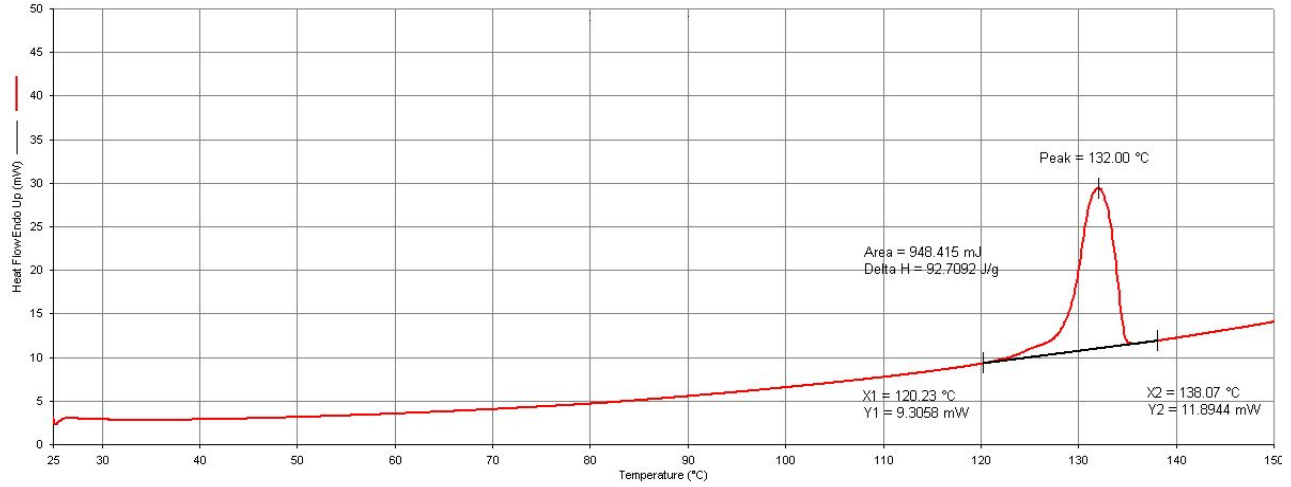

(b)

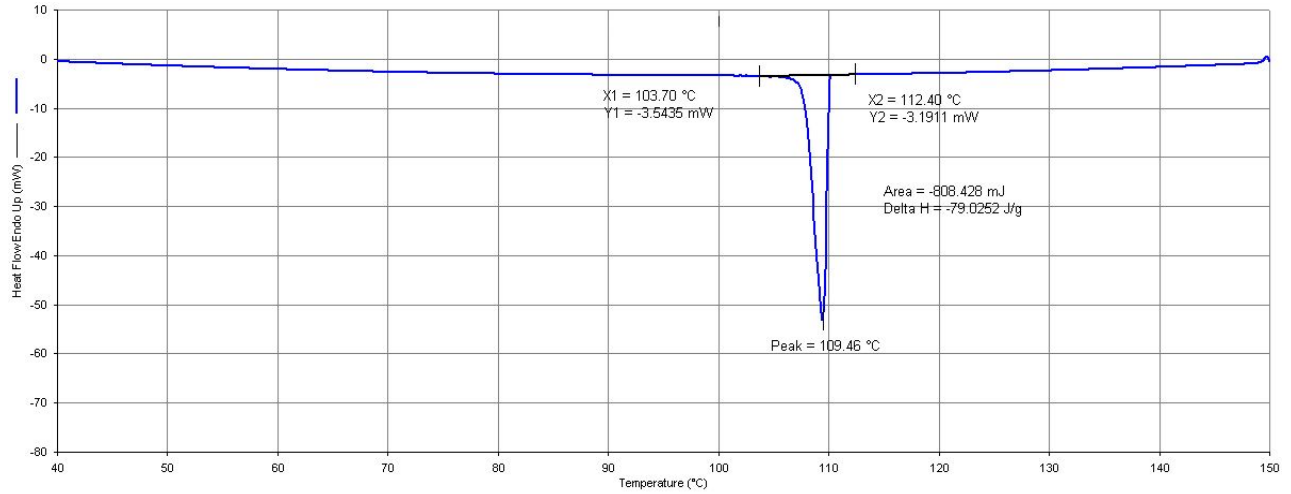

(c)

Figure S6. Thermal analyses for R-[QH]MS: (a) TGA thermogram, (b) DSC, heating cycle and (c) DSC trace, cooling cycle.

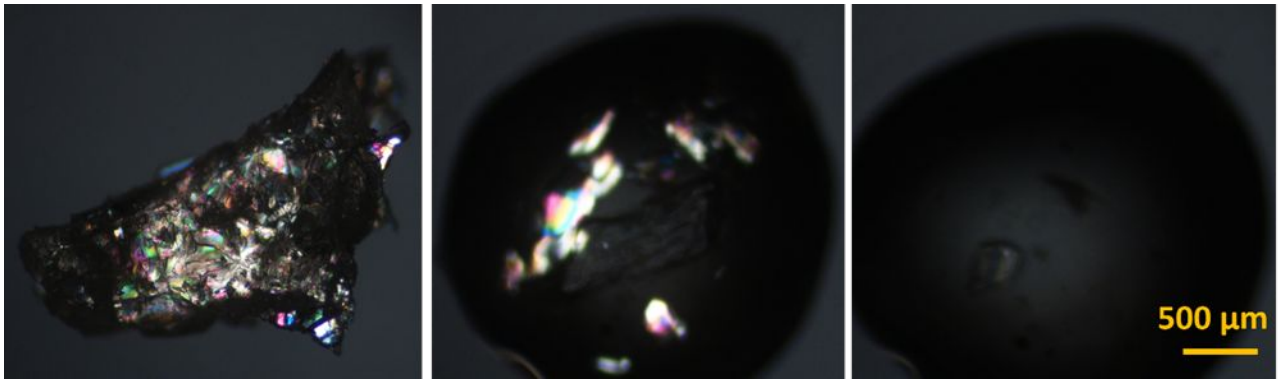

Figure S7. Cross-polarized HSM pictures of a [QHrac]MS single taken during the transition occurring at 150°C that clearly indicate the melting of the compound.

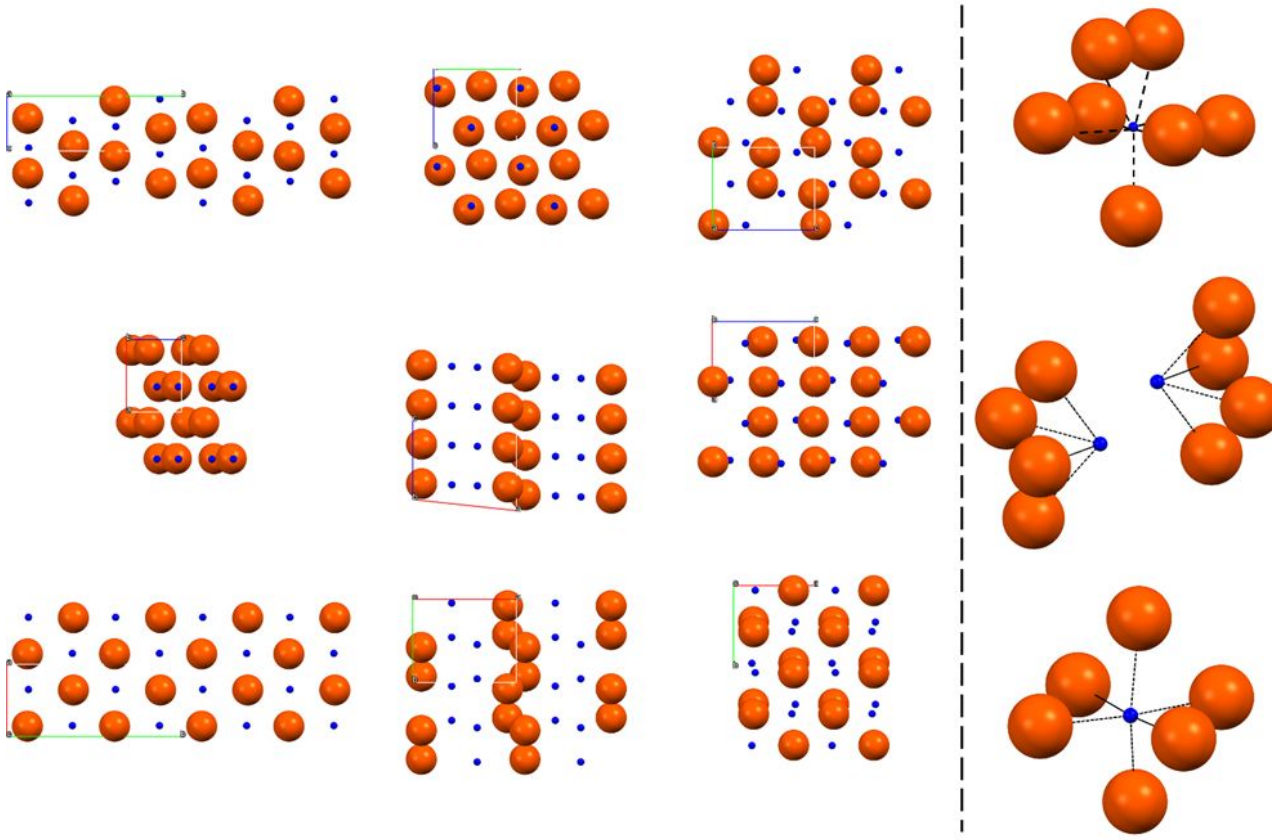

Figure S8. Left, crystal packing of [QHco]MS, the racemic [QHrac]MS, and enantiopure R-[QH]MS viewed down the a-axis (top) b-axis (middle) and c-axis (bottom). Right, representation of the ionic environments detected within: (a) the achiral [QHco]MS, (b) racemic [QHrac]MS, and (c) enantiopure R-[QH]MS. The cations and anions are depicted as blue and red spheres, respectively.

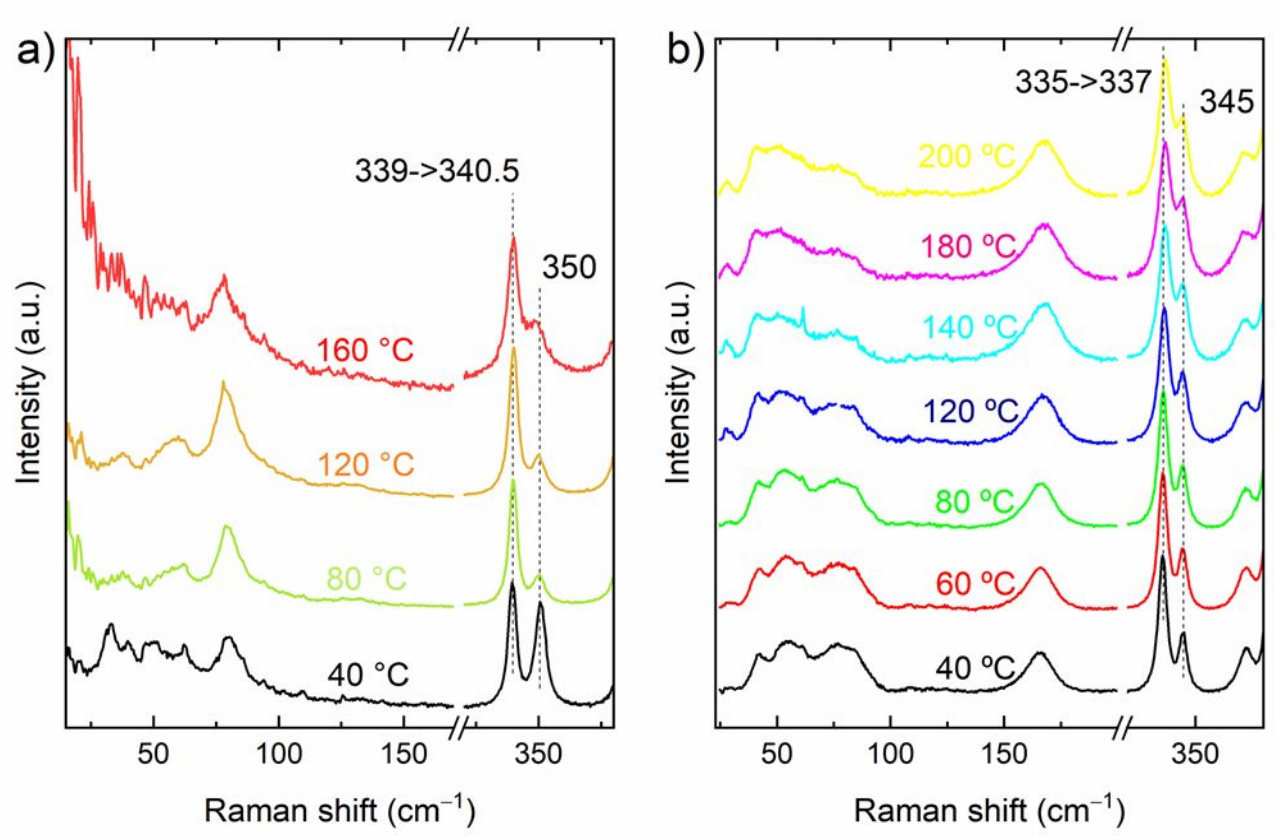

Figure S9. Variable temperature spectra for (a) the racemic [QHrac]MS and (b) the achiral [QHco]MS compounds.

.

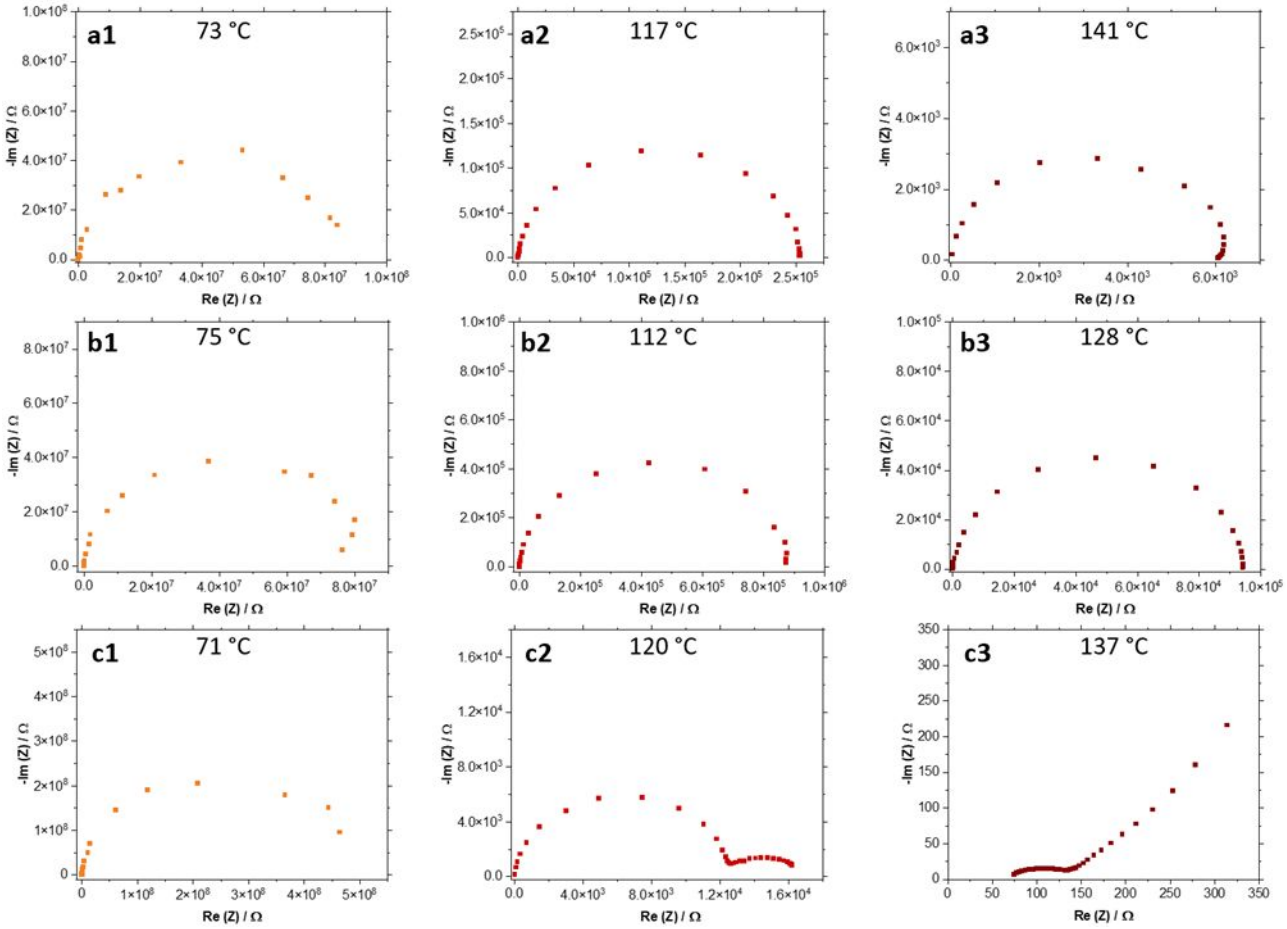

Figure S10. Evolution of the Nyquist plots at increased temperatures of [QHrac]MS (a1, a2, and a3), [QHco]MS (b1, b2, and b3), and R-[QH]MS (c1, c2, and c3).

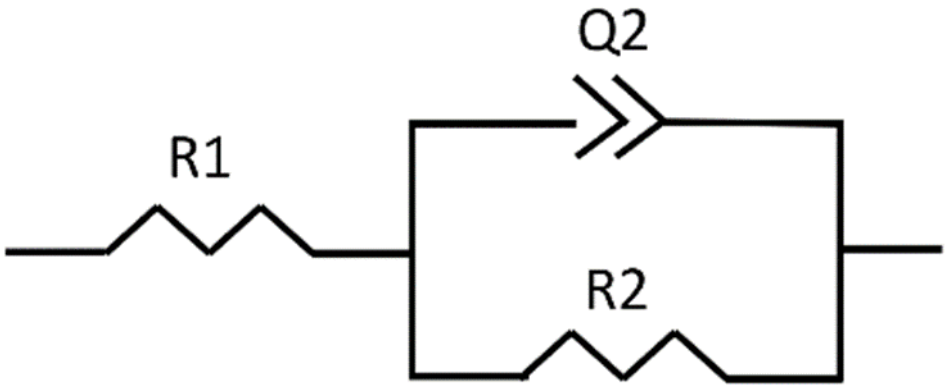

Figure S11. Equivalent circuit used for fitting the electrochemical impedance spectra: R1 is related to the electronic resistance of the cell (cables, blocking electrodes); R2 is the bulk ionic resistance of the pellet, and Q2 is the constant phase element that describes the double layer capacitance at the two ionic conductor/blocking electrode interfaces.

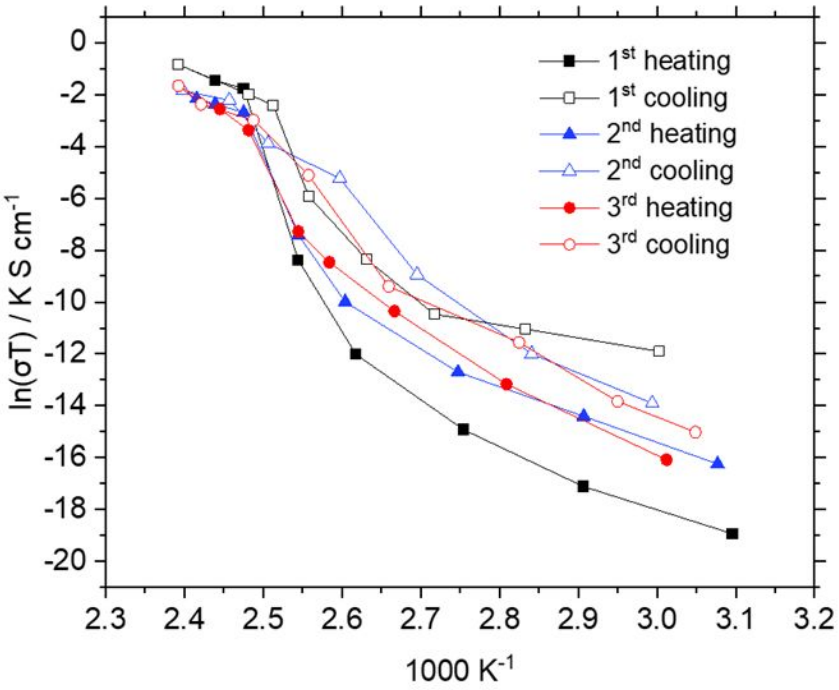

Figure S12. Arrhenius plots of enantiopure R-[QH]MS in three cycles of heating and cooling.

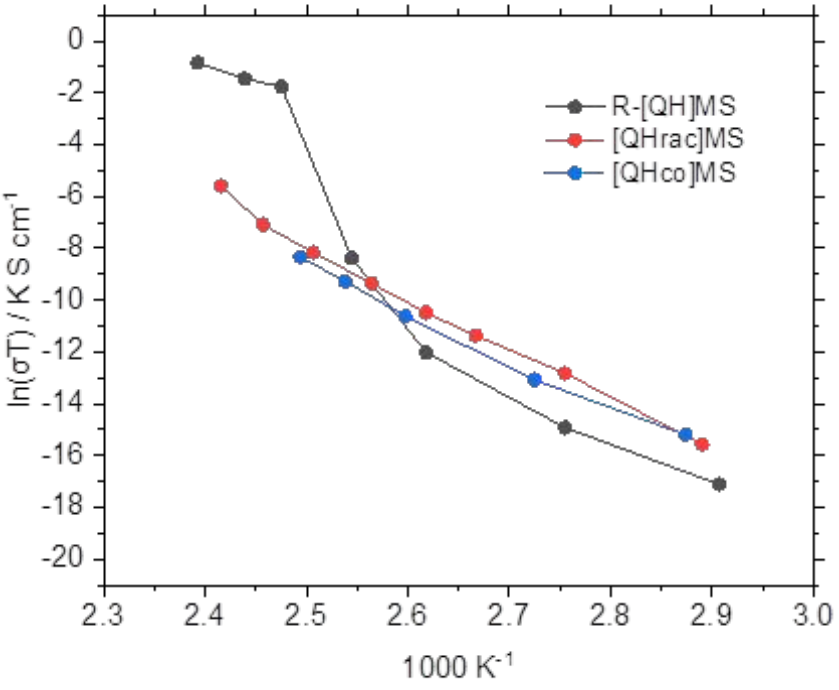

Figure S13. Arrhenius plots of R-[QH]MS, [QHrac]MS, and [QHco]MS.